

Supporting Information for:

The Effect of a Common Purification Procedure on the Chemical Composition of the Surfaces of CdSe Quantum Dots Synthesized with Trioctylphosphine Oxide (TOPO)

*Adam J. Morris-Cohen, Martin D. Donakowski, Kathryn E. Knowles, and Emily A. Weiss**

Department of Chemistry, Northwestern University, 2145 Sheridan Rd., Evanston, IL 60208-3113

*corresponding author. Ph: 847-491-3095.Fax: 847-491-7713.Email: e-weiss@northwestern.edu

EXPERIMENTAL METHODS

Synthesis of CdSe QDs. We synthesized 3.1-nm CdSe QDs with a procedure adapted from Qu, et al.¹ We added either 90% or 99% TOPO (1.94 g, 5.02 mmol), HDA (1.94 g, 8.03 mmol), and cadmium stearate (0.112 g, 0.165 mmol) to a dry 50-mL three-neck round bottom flask and heated the mixture to 105°C while stirring under positive nitrogen flow to remove water from the reagents. After 40 minutes, we increased the temperature to 320 °C. After the cadmium stearate dissolved to form an optically clear solution, we rapidly injected trioctylphosphine selenide (TOPSe, 1 mL of 1 M solution in TOP, prepared and stored in a glovebox). Holding the temperature at 290 °C for 1 minute produced a bright red solution, which was rapidly cooled by adding 5 mL of chloroform under positive nitrogen flow. The chloroform/QD mixture sat unstirred for ~2 hours before purification, during which time some excess free ligand

precipitated. We decanted the supernate from the precipitated ligand and purified the resulting solution according to the procedure described in the text.

Measurement of UV-Vis Absorbance Spectra. We performed UV-visible absorption measurements on a Varian Cary 5000 spectrometer using 1-cm quartz cuvettes, and corrected the baselines of all spectra with neat solvent prior to measurement.

Transmission Electron Microscopy. We prepared samples for TEM by applying a single drop of ~10- μ M solution of QDs in chloroform onto an ultrathin holey carbon-coated copper TEM grid (Ted Pella). We allowed the solvent to evaporate from the grid under ambient conditions. We observed the samples using a Jeol JEM-2100 TEM with a 200-kV beam energy. Analysis of the TEM images with *ImageJ* software² showed the mean diameter of the QDs was 3.1 ± 0.2 nm.

Energy Dispersive Spectroscopy (EDS). *SEM.* To prepare samples for EDS analysis, we dropcast QDs from chloroform solutions onto silicon wafers. We applied four to eight drops of a sample successively to a wafer and allowed sufficient time between each drop for the solvent to evaporate. Prior to analysis, we stored the samples under vacuum to reduce oxidation and contamination. A ~5-nm carbon coating deposited on top of the QD film prevented the samples from charging during analysis. We used the secondary electron detection mode to perform elemental analysis on films made from samples PS-1 through PS-4. We acquired spectra over regions on the QD films between 50 and 250 μm^2 in area. The beam energy was 20 kV and the spectral window was 0 to 10 keV. The QD films were inhomogeneous over microns with thick islands of QDs in some places and apparently bare substrate in others; we selected areas in the film to sample from that showed a strong Cd and Se signal from the QDs (nearly equal to or greater than that of the Si from the substrate) .

STEM. Scanning transmission electron micrographs were acquired on a Hitachi HD-2300 STEM using ultrathin holey carbon-coated copper grids (Ted Pella) with a beam energy of 120 kV.

ICP-AES. We added ~25 nanomoles of CdSe QDs dispersed in chloroform from each sample PS-1 through PS-4 to a glass scintillation vial and dried the samples using a stream of N₂(g). We added 2 mL of either room temperature or 45 °C aqua regia (concentrated HCl: glacial HNO₃, 3:1 v/v) to each vial and allowed the samples to digest for 2 hrs. Preparation of samples with 45 °C and room temperature aqua regia produced P:Cd ratios that agreed within 12% on average and we present an average of all four measurements. We diluted the solution in μ -pore-filtered water to a concentration of 5% aqua regia and approximately 5 ppm Cd, Se and P. We calibrated the instrument with the ICP standards phosphoric acid (1,000 mg/L P in H₂O, TraceSELECT[®] Ultra, Aldrich), Se (1,000 mg/L Se in 2% HNO₃, Aldrich) and Cd (1000 mg/L Cd in 2% HNO₃, Aldrich).

X-ray Photoelectron Spectra and Modification of the XPS Sensitivity Factors to Account for the Heterogeneity of QD Films. Scans were taken with an Al anode (1486.6 eV) driven at 225 W. We collected survey scans from binding energies of 0 - 1100 eV. For survey scans and details scans of the P(2p), Cd(3d), C(1s) and N(1s) regions, we used a pass energy of 70 eV. Typical collection times were 10 minutes for the survey scans and 8 minutes for each of the detail scans. We averaged the detail scans over three traces of the region and analyzed four different spots on each sample. All measurements were taken at a pressure $<3 \times 10^{-9}$ mbar. The typical beam energy and emission current of the electron gun were 10 eV and 7 μ A, respectively.

In a homogeneous sample, the intensity of a peak in an XP spectrum is given by eq. 1, where

$$I = n f \beta \sigma \theta y A T = n S \quad (1)$$

I is the intensity of the peak, n is the number of atoms per unit volume, f is the flux of X-rays through the sample, β is the escape depth, which describes how quickly the probability of escape for an emitted electron decays as the depth from which it is emitted increases, σ is the photoelectric cross section, θ is an angular factor related to the geometry of the detector, source and sample, y is the efficiency of forming electrons with the full kinetic energy, A is the area probed and T is the efficiency of the detector.^{3,4} Typically, $(f\beta\sigma\theta yAT)$ are together called the sensitivity factor, S . Sensitivity factors for each element are found experimentally and vary from instrument to instrument, but are constant for a single instrumental setup. Relative ratios of elemental concentrations can be calculated using eq. 2, where n_x is the number density per unit

$$\frac{n_a}{n_b} = \frac{I_a/S_a}{I_b/S_b} \quad (2)$$

volume of a given element x .

In a homogeneous sample, β is defined by eq. 3. It is the probability of escape for a photoelectron at a given kinetic energy (KE) from depth z , integrated over the entire thickness of

$$\beta = \int_0^d \exp\left(-\frac{z}{\lambda}\right) dz \quad (3)$$

the sample, d . If KE is sufficiently high, $\lambda = 0.5(KE)^2$.⁵ In a typical XPS experiment, λ is on the order of several nanometers. For thick samples where d is much greater than λ , the integral in eq. 3 equals λ ($\beta = \lambda$), and λ appears in the sensitivity factor.

Films of QDs are heterogeneous: the probability of an electron escaping from the sample depends on the element and spatial region from which it originates. For example, the C atoms on the ligands coordinated to the QD are much more likely to be near the surface than are the Cd and Se atoms in the core of the QD (Figure S1A); thus photoelectrons generated in C atoms are more likely to escape into vacuum than are photoelectrons generated in Cd and Se atoms. To

account for the heterogeneity of the sample, we corrected the sensitivity factor using the method described by Nanda et al. with slight modifications.⁵ We integrated the probability of escape for photoelectrons generated from each element of interest over the entire volume in which the element is found. For any given photoelectron, the probability of reaching the detector decreases as the distance it must travel through solid matrix increases. The distance an electron must travel through the QD film in the direction of the detector before it escapes into vacuum is given by $f(r, \phi)$, Figure S1B, eq. 4. In eq. 4, the z term from eq. 3 has been replaced by $f(r, \phi)$.

$$\beta = \int_{R'}^{R''} \int_0^\pi \int_0^{2\pi} \exp - \frac{(f(r, \phi))}{\lambda_{KE}} r^2 \sin(\phi) dr d\phi d\theta \quad (4)$$

Additionally, the one-dimensional integral with respect to depth (z) has been converted into a three dimensional integral in spherical coordinates with the origin at the center of the QD. Figure S1B shows a schematic diagram illustrating the relevant trigonometric segments and the caption contains the equation for $f(r, \phi)$. We calculated the integral in Mathematica using limits (R' and R'') determined by the region in which a particular element likely exists, as illustrated in Figure S1A. We calculated β for each element in the volumes they occupied using eq. 4, modified the sensitivity factor by replacing λ with β in eq. 1, and then calculated elemental ratios for P, N and Cd using eq. 2.

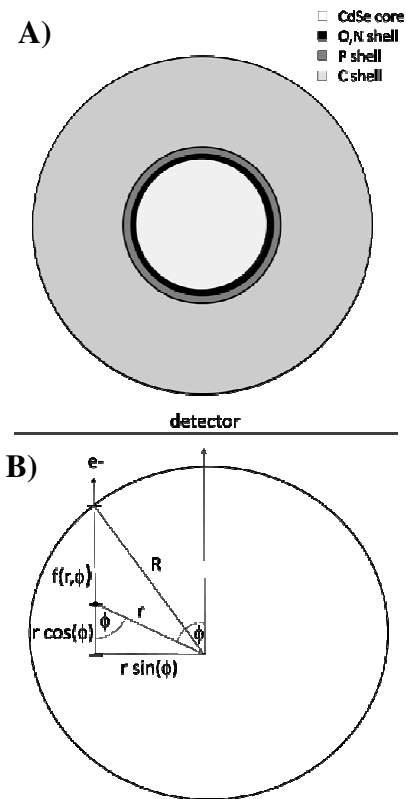


Figure S1. A) Schematic diagram of a QD-ligand complex (QD-L). We integrated the P and (N) signal over a spherical shell with a width, Δr , equal to 0.22 nm (0.14 nm) (the covalent diameter of phosphorus (nitrogen)) and separated from the QD by 0.15 nm in the case of P to account for the covalent diameter of oxygen. The black line in part (A) represents the area occupied by oxygen between the CdSe core (green) and P shell (dark gray). **B)** Graphical representation of the distance an electron must travel until it escapes into vacuum as a function of its location in the QD: $f(r, \phi) = (R^2 - r^2 \sin^2(\phi))^{1/2} - r \cos(\phi)$. Here, R is the radius of the QD-L complex from the center of the QD to the outer edge of the ligand shell, r is a vector from the center of the QD to the differential volume, dv , from which the photoelectron originates, and ϕ is the angle between r and the vector from the center of the QD to the detector. The distance $f(r, \phi)$ does not depend on θ because of the assumed spherical symmetry of the QD.

Ligand Exchange. To prepare CdSe QDs with a high density of OPA ligands for XPS analysis, we added 10^4 molar equivalents (0.0392 g) of OPA to 4 mL of a 2.02×10^{-5} -M solution of QDs synthesized with 99% TOPO and dispersed in chloroform. We refluxed this solution

while stirring for 12 hours under nitrogen atmosphere, and separated the QDs from excess OPA by precipitating the QDs with 10 mL of methanol, centrifuging the turbid liquid to form a red pellet, and decanting the clear supernatant liquid containing excess OPA. We redispersed the pellet containing the QDs in 5 mL of chloroform and used immediately.

Ligand Exchange Procedure for ^{31}P NMR Experiments. We prepared a 0.95 M stock solution of propionic acid (Aldrich) and Triton B (benzyl(trimethyl)ammonium hydroxide, Aldrich) in methanol; the Triton B both deprotonates the propionic acid to form the X-type ligand propionate, and solubilizes the salt in chloroform. We performed the ligand exchange with 250 μL (2×10^3 propionate:QD), 500 μL (4×10^3 propionate:QD), and 1000 μL (8×10^3 propionate:QD), of the propionate stock solution. The sample with 500 μL of propionate stock solution exchanged the greatest number of ligands from the surface of the QD without degrading the samples. Treating the QDs with 1000 μL of propionate stock solution produced black and orange precipitates of aggregated QDs and insoluble ligands. We were unable to form homogeneous dispersions of these samples in the NMR tubes. Treatment of the QDs with 250 μL of propionate stock solution yielded lower concentrations of P-ligands after exchange than did treatment with 500 μL of propionate solution. Comparison of the UV-Vis absorption spectra of the QDs before and after ligand exchange showed that the concentration of QDs decreased consistently (for samples from all purification steps) by a factor of ~ 2.5 after treatment with 4000 propionate:QD. We attribute the decrease in concentration to the reduced solubility of the QDs in chloroform after exchange.

³¹P NMR Analysis of the Supernates from Each Purification Step.

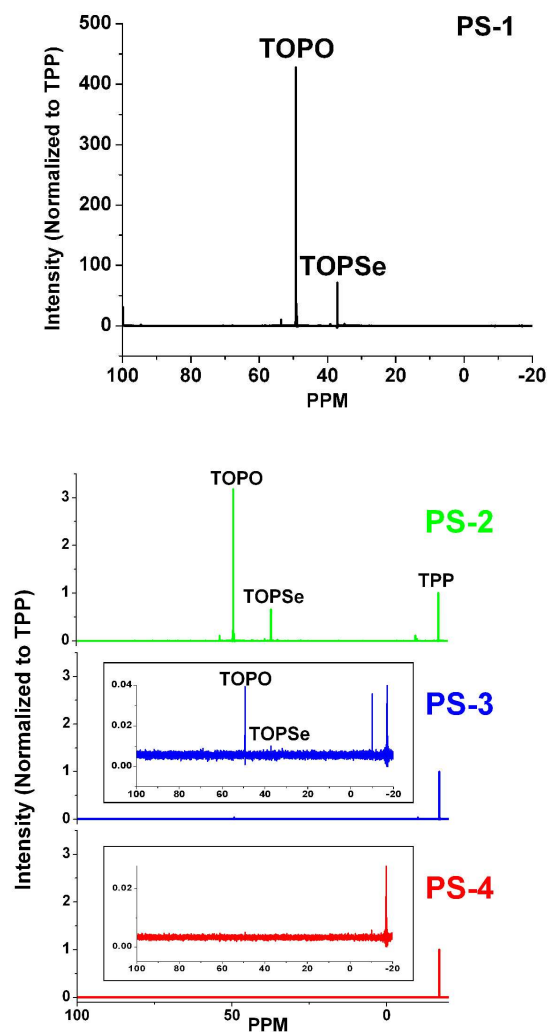


Figure S2. ³¹P NMR spectra of the supernates from purification steps PS-1 – PS-4. The resonance at -17 ppm is the integration standard, triphenylphosphate (TPP), to which the other signals in the spectrum are normalized. In addition to the labeled peaks, the peak at -9.7 ppm is the degradation product of TPP (see Figure 6 in the main text).

Calculation of Photoluminescence Quantum Yield. We calculated the PL quantum yields of the solutions of QDs, Φ_{QD} , for PS-1 through PS-4 using eq. 5,⁶ where $\Phi_r = 0.95$ is the

$$\Phi_{QD} = \Phi_r \left(\frac{a_r}{a_{QD}} \right) \left(\frac{I_{QD}}{I_r} \right) \left(\frac{n_r^2}{n_{QD}^2} \right) \quad (5)$$

PL quantum yield of rhodamine 6G, a_x is the absorbance of species x at the excitation wavelength (510 nm), I_x is the integrated PL intensity of species x , and n_x is the refractive index of the solvent in which the PL was measured at room temperature. We measured the PL of rhodamine 6G in ethanol ($n = 1.359$), and the PL of the QDs in hexane ($n = 1.372$).

Cd:Se Ratio as a Function of Diameter for Several Samples of CdSe QDs.

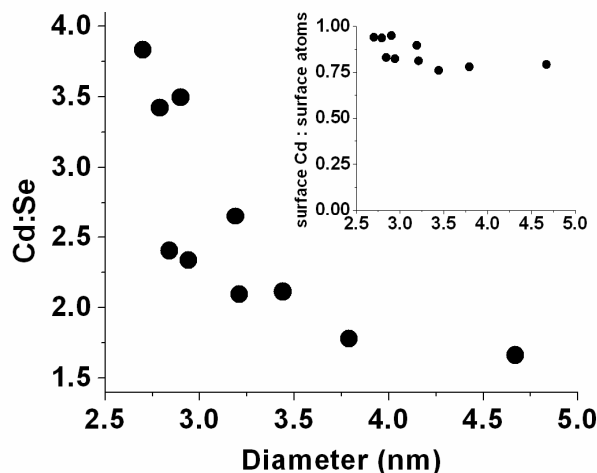
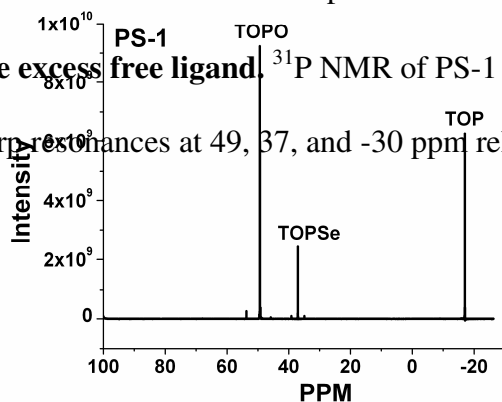


Figure S3. A) Plot of the Cd:Se ratio as a function of QD diameter. The Cd:Se ratio was measured using ICP-AES following digestion of the QDs in aqua regia. The diameters listed on the x-axis are calculated from the energies of the band-edge ground state absorptions of the QDs in CHCl_3 , not from TEM, because we did not obtain TEM images of each size. Note that the QDs used in this study are 3.1 nm by TEM, but 2.9 nm by UV-Vis absorption, and therefore plotted as 2.9-nm QDs in this figure. **(Inset):** The ratio of surface Cd atoms to total surface atoms as a function of diameter calculated using the Cd:Se ratios in the main plot, and assuming a 1:1 stoichiometry for the core and a surface depth of 0.4 nm (1.5 Cd-Se bond lengths).

PS-1 samples have excess free ligand. ^{31}P NMR of PS-1 QDs (before exchange with propionate) shows sharp resonances at 49, 37, and -30 ppm relative to phosphoric acid, Figure



S4. These resonances have been identified previously as free TOPO, TOPSe and TOP, respectively.^{7,8} Using triphenyl phosphate as an internal integration standard, we calculated that free TOPO and TOPSe are present in PS-1 at total concentrations ranging from 100/QD to 1000/QD, depending on the particular batch. At PS-1, we also observe a weaker resonance at 54 ppm that has been identified as *n*-octyl di-*n*-octylphosphinate⁹ and is present as an impurity in 90% TOPO. This resonance does not appear in PS-2, 3, or 4.

Figure S4. ³¹P NMR spectrum of the PS-1 sample of QDs synthesized with 90% TOPO as the coordinating solvent. Peaks are referenced to phosphoric acid.

¹H NMR Analysis of Reference Compounds. Figure S5 shows the ¹H NMR spectra (in CDCl₃) of cadmium stearate and stearic acid (**A**); an amide formed by bringing a mixture of HDA and cadmium stearate to 320 °C, immediately cooling the reaction to room temperature, and filtering off the cadmium oxide side product (**B**); and propionate and Triton B, the solution used to exchange off the ligands bound to the QDs, octylphosphonic acid, and triphenylphosphate (the integration standard used for ³¹P NMR) (**C**).

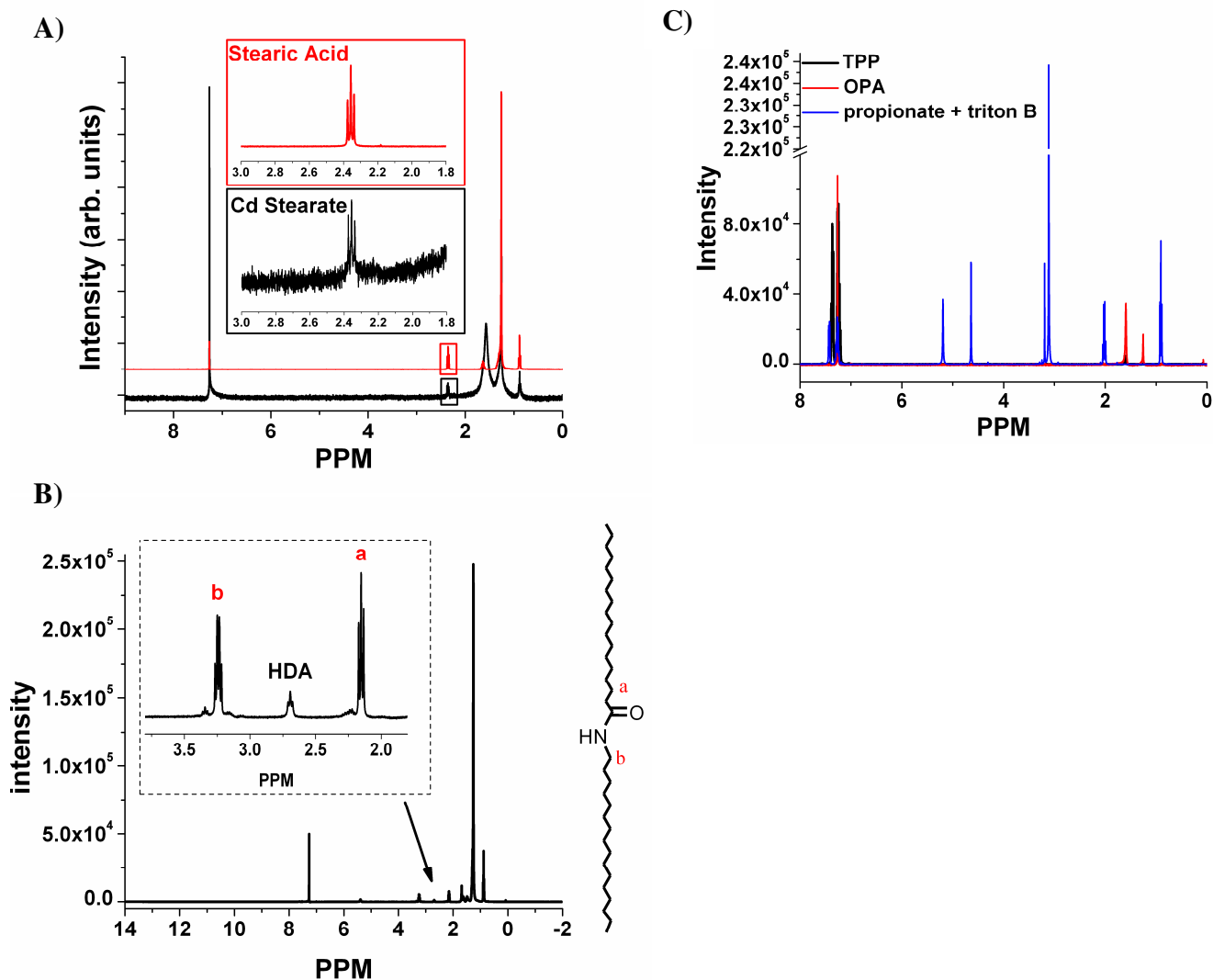


Figure S5. A) ^1H NMR spectra of cadmium stearate (black) and stearic acid (red) in CDCl_3 . The triplets at 2.35 ppm correspond to the methylene protons on the carbon adjacent to the carboxylic acid group. B) ^1H NMR (in CDCl_3) of the amide formed (structure is drawn on the spectrum) by bringing a mixture of cadmium stearate (0.28 g, 0.41 mmol) and HDA (0.50 g, 2.1 mmol) to 320 $^\circ\text{C}$ under nitrogen, immediately removing it from heat, quenching with chloroform when it reached 220 $^\circ\text{C}$, and centrifuging the resulting suspension to collect a dark brown pellet (CdO) and a clear supernatant. We evaporated the solvent from the supernatant to produce a white powder, which we characterized by ^1H NMR. This compound is not soluble in methanol, and therefore it precipitates with the QDs as free ligand during the purification procedure. C) ^1H

NMR (in CDCl_3) of triphenylphosphate, octylphosphonic acid, and a mixture of propionic acid and the base Triton B, which deprotonates the acid to form propionate.

Characterization of QDs Synthesized with 99% TOPO. Figure S6 shows the UV-Vis absorption spectrum of CdSe QDs synthesized with the procedure outlined above, but with 99% TOPO instead of 90% TOPO. The QDs have a band-edge absorption maximum of $\lambda = 594$ nm; this wavelength corresponds to a diameter of 4.3 nm. Figure S7 shows the ^1H NMR of these QDs, purified to PS-2. This spectrum shows the presence of free amide, formed upon the reaction of HDA with cadmium stearate (Figure S5B), and two broad signals at 2.85 ppm and 2.33 ppm that we assign to bound HDA and bound stearate, respectively.

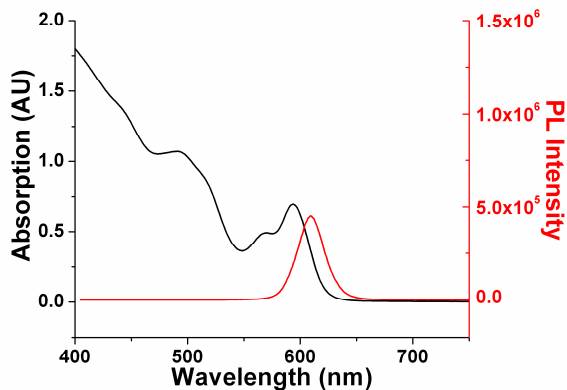


Figure S6. UV-Vis absorption spectrum of PS-3 CdSe QDs synthesized with 99% TOPO. The band-edge absorption is at 594 nm, and the PL maximum is at 604 nm. The QDs are approximately 4.3 nm in diameter, which is larger than the QDs prepared with an identical procedure, but with 90% TOPO rather than 99% TOPO. The presence of strongly-binding impurities in 90% TOPO (including OPA) probably arrests the growth of the QDs.

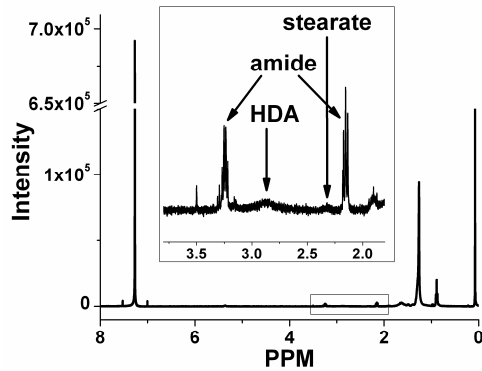


Figure S7. ^1H NMR of CdSe QDs synthesized with 99% TOPO and purified to PS-2.

The decrease of PL upon purification is only partially reversible by addition of free ligand.

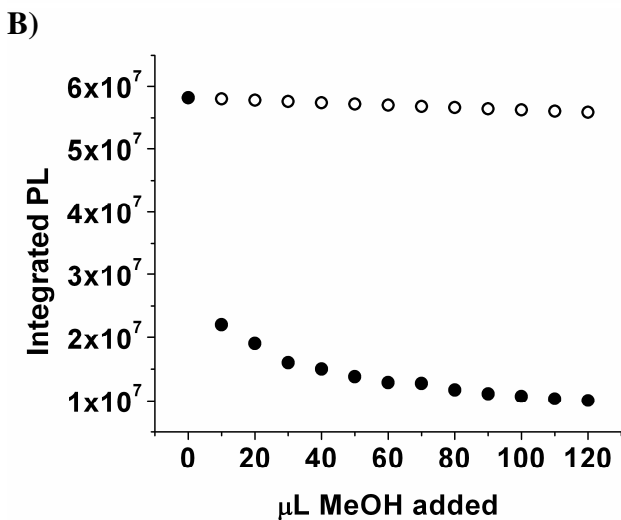
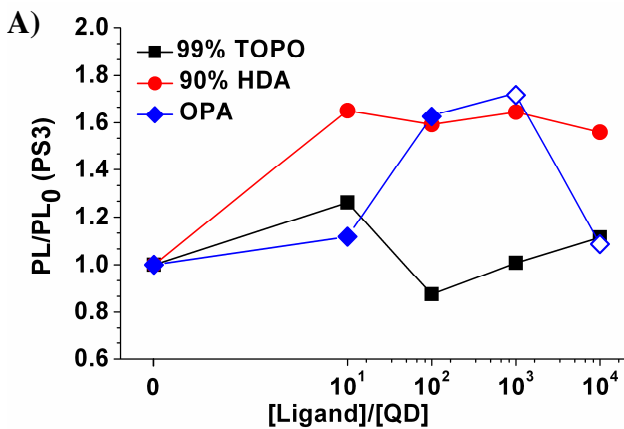


Figure S8. A) Plot of the PL of PS-3 QDs after stirring in various concentrations of added HDA, TOPO, and OPA ligand in distilled CHCl_3 for 24 hrs. Values are plotted relative to a PS-3 sample without any added ligand. The value of PL/PL_0 for PS-2 QDs would be ~ 3.0 on this plot. The points for OPA at 10^3 and 10^4 ligands/QD are marked with open diamonds because the QDs in these samples were degraded by OPA—that is, the maximum of their first absorption peaks shifted from 531 nm to 529 nm at 10^3 OPA ligands/QD, and to 520 nm at 10^4 OPA ligands/QD.

B) Integrated PL intensity of a sample of PS-2 QDs upon addition of successive 10- μL aliquots of methanol (solid circles). The open circles are the calculated PL intensities that would result from dilution of the sample by an inert solvent (rather than methanol). For reference, addition of 50 μL of methanol results in a molar ratio of 8×10^5 :1 methanol:QD.

Table S1. Fractional Surface Coverage of P-containing Ligands for a 3.1-nm CdSe QD with a P:Cd ratio of 0.62 (PS-3), Calculated for Different Cd:Se ratios.

Cd:Se ratio	Surface Cd:Se	number of P-containing ligands / QD ^b	number of P-containing ligands / surface atom ^a	number of P-containing ligands / surface Cd
1	141:141	150	0.53	1.07
1.25	167:114	166	0.59	0.99
1.5	189:92	180	0.64	0.95
1.75	206:75	191	0.68	0.92
2	221:60	200	0.71	0.90
2.5	244:37	214	0.76	0.88
3	261:20	225	0.80	0.86
3.5	274:7	233	0.83	0.85

^aTotal surface atoms equals number of surface cadmium atoms plus number of surface selenium atoms.

References.

- (1) Qu, L.; Peng, X. *J. Am. Chem. Soc.* **2002**, *124*, 2049-2055.
- (2) Rasband, W. S., *ImageJ*, U. S. National Institutes of Health, Bethesda, Maryland, USA, **1997-2009**.
- (3) Wagner, C. D. *Handbook of X-ray Photoelectron Spectroscopy*; Perkin-Elmer Corporation: Eden Prairie, 1979.
- (4) Katari, J. E. B.; Colvin, V. L.; Alivisatos, A. P. *J. Phys. Chem.* **1994**, *98*, 4109-4117.
- (5) Nanda, J.; Kuruvilla, B. A.; Sarma, D. D. *Phys. Rev. B* **1999**, *59*, 7473-7479.
- (6) Crosby, G. A.; Demas, J. N. *J. Phys. Chem.* **2002**, *75*, 991-1024.
- (7) Kopping, J. T.; Patten, T. E. *J. Am. Chem. Soc.* **2008**, *130*, 5689-5698.
- (8) Wang, F.; Yu, H.; Li, J.; Hang, Q.; Zemlyanov, D.; Gibbons, P. C.; Wang; Janes, D. B.; Buhro, W. E. *J. Am. Chem. Soc.* **2007**, *129*, 14327-14335.
- (9) Wang, F.; Tang, R.; Kao, J. L. F.; Dingman, S. D.; Buhro, W. E. *J. Am. Chem. Soc.* **2009**, *131*, 4983-4994.